

A Multifunctional Sensor Node Sharing Coils in Wireless Power Supply, Wireless Communication and Distance Sensing Modes

Ryo Shirai* Tetsuya Hirose† Masanori Hashimoto*

* Dept. of Information Systems Engineering, Osaka University Email: { shirai.ryo, hasimoto } @ist.osaka-u.ac.jp

† Dept. of Electrical and Electronics Engineering, Kobe University Email: hirose@eedept.kobe-u.ac.jp

Abstract—This paper proposes a multifunctional sensor node that shares coils for wireless power supply (WPS), wireless communication, and distance sensing functions to pursue a small volume implementation. The sensor node has two coils inside, which are used as an antenna in WPS mode and wireless communication mode. In distance sensing mode, on the other hand, the two coils are used as electrodes to radiate an electric field to neighboring nodes. For switching functions, a normally-on junction type FET (JFET) is introduced so that the node automatically enters into the WPS mode when no energy is left in the node. We evaluated the functionalities and performance of each mode with a prototype. Experimental results show that, in the WPS mode, the two coils are automatically connected to each other, and the node can receive power even if there is no energy left in the node. In the wireless communication mode, 1 kbps communication is possible at a distance of 10 cm. Also, the distance can be measured at a range of 30 mm or less by using two coils as electrodes.

I. INTRODUCTION

Applications incorporating IoT and smart city concepts are widespread in recent years [1][2], but a restriction on the installation location of sensor nodes prevents some applications from being actualized. For eliminating this restriction, small-volume maintenance-free sensor nodes that can transmit information through wireless communication are highly demanded. To realize a maintenance-free tiny sensor node that can be installed anywhere, the sensor node needs to have wireless power supply (WPS) or energy harvesting functions in addition to the sensing function. With those functions, sensor nodes are expected to last almost indefinitely [3][4]. A challenge to the node implementation is that multiple functionalities need to be implemented in a very small volume. Fortunately, it has become possible to perform arithmetic processing in small sensor nodes thanks to aggressive VLSI scaling. However, it is still difficult to accommodate antennas and coils required by analog circuits in a small volume.

We have proposed a system named “iClay”(Fig. 1)[5], which uses numerous tiny sensor nodes. The iClay system is supposed to provide instant real-time 3D modeling with the clay, in which small sensor nodes are embedded. Each sensor node in the clay obtains energy through WPS, measures the distance to the neighboring node, and transmits the distance information to the host computer by wireless communication function. The host computer reproduces the shape of the clay based on the obtained distance information. For actuating this particular application of iClay, we have to establish WPS, wireless communication, inter-node distance sensing, and clay shape reconstruction.

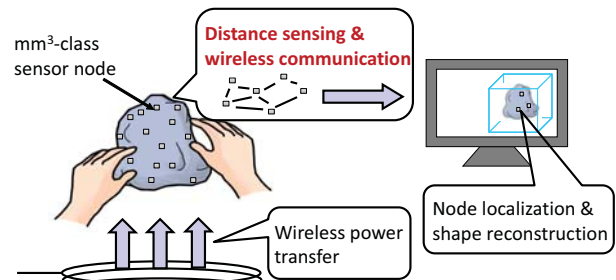


Fig. 1. iClay system.

For shape reconstruction, a cross-entropy based node localization method is developed in [6] and its parallel computation efficiency is presented in [7]. Ref. [8] demonstrated wireless power transfer of 450 μW to a 50mm³ node. Ref. [9] discusses the coil design at the power transmitter side and designs a wireless power transfer system. As for inter-node distance sensing, [5] and [10] show that cm-scale communication can be achieved by capacitive coupling based communication. Tiny dedicated antenna less transmitter proposed in [11] can be used as a small volume wireless communication system in iClay system.

This paper focuses on the implementation of iClay sensor nodes. The most challenging requirement is mm³-class volume, which prevents the simultaneous accommodation of an antenna for wireless communication, a receiving coil for WPS, and electrodes for distance sensing. In [10], a dual-use antenna for wireless communication and distance sensing is proposed. However, there has been no discussion about the overall node implementation including a circuit for communication, a voltage boosting circuit for distance sensing, and a circuit for WPS. Therefore, in this paper, we propose a small volume implementation of the iClay node that shares two coils among WPS, wireless communication, and inter-node distance sensing functions, and evaluate the functionalities and performance of the implemented prototype.

II. PROPOSED SENSOR NODE STRUCTURE

Fig. 2 shows the schematic of the proposed sensor node, and Figs. 3 and 4 show the prototype of the proposed sensor node. The prototype sensor node is implemented with discrete components, and the volume of the node is exactly 10mm \times 10mm \times 10mm. The sensor node is composed of two spiral coils and a circuit board as shown in Fig. 4. These two spiral coils correspond to L1 and L2 in Fig. 2, and they are shared

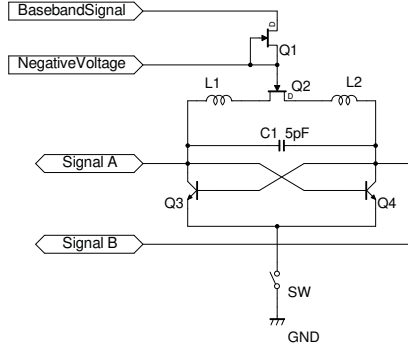


Fig. 2. Proposed sensor node.

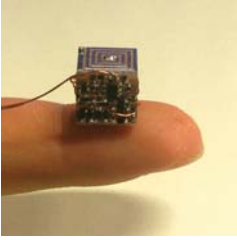


Fig. 3. Prototype sensor node. Fig. 4. Expanded view of sensor node.

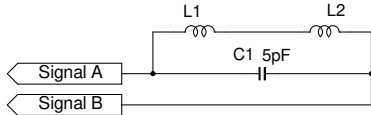


Fig. 5. Equivalent circuit of WPT mode.

by the functions of WPS, wireless communication, and inter-node distance sensing. The function switching is enabled by the switch (SW) and Q2, which will be explained below.

A. Wireless Power Supply Mode

In WPS mode, Q2 is in ON state, and then L1 and L2 compose series-connected power receiving coils. Also, the bottom switch SW is OFF. In this case, the equivalent circuit of WPS mode becomes Fig. 5. When an alternating magnetic field is given to the coils, electromagnetic induction phenomenon occurs, and energy can be obtained from “Signal A” and “Signal B” terminals in Fig. 2.

The iClay sensor node operates using the stored energy obtained through WPS. Therefore, the node should be in WPS mode when there is no energy left in the node. Besides, MOSFETs are often used as a switch of, for example, Q2. However, MOSFET is a normally-off switching element that becomes on when a voltage is applied to the gate terminal, and hence the switch cannot be on when the inner node energy is running out. To solve this issue, we use a normally-on JFET as Q2 in Fig. 2. The JFET has a feature that the channel between drain and source conducts when the applied voltage to the gate is 0V. When the node is out of energy, the voltage applied to Q2 vanishes and Q2 becomes ON state, and therefore the two coils L1 and L2 are connected to each other, and the node enters the WPS mode.

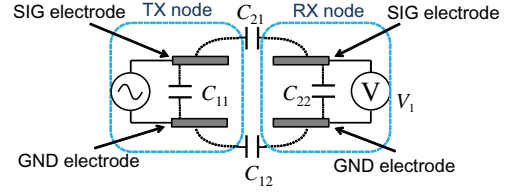


Fig. 6. Distance sensing based on capacitive coupling.

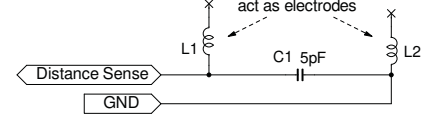


Fig. 7. Equivalent circuit of distance sensing mode.

B. Distance Sensing Mode

The node measures the distance to its neighboring node once the energy is stored in the node. For sensing distance between nodes, we use capacitive coupling based distance sensing method proposed in [5]. In this case, both the TX and RX nodes should be equipped with two electrodes: SIG electrode and GND electrode as shown in Fig. 6. When these nodes approach each other, parasitic capacitances of C_{11} , C_{12} , C_{21} , and C_{22} arise as shown in Fig. 6. When the TX node injects an alternating current between the electrodes, a current also flows in the RX node through the parasitic capacitances. Then, the RX node can estimate the distance from TX node by measuring the voltage between the electrodes since the capacitances of C_{12} and C_{21} depend on the distance between the nodes.

The proposed structure uses the two spiral coils as two electrodes referring to [10], where [10] presents an idea that uses a spiral coil as an electrode and validates the idea through hardware measurement. To use the spiral coil as an electrode, we need to disconnect L1 and L2 electrically. In the structure of Fig. 2, L1 and L2 can be disconnected by assigning OFF state to Q2, and then the sensor node enters to the distance sensing mode (Fig. 7). Q2 is an N channel JFET, and hence a negative voltage is required to turn off Q2, where the negative voltage generation will be discussed later. When the SW in Fig. 2 is opened and a negative voltage of -5V is applied to the gate of Q2, the circuit of Fig. 2 can be equivalently redrawn as Fig. 7. In Fig. 7, one of L1 and L2 can be regarded as the SIG electrode, and the other can be regarded as the GND electrode. The TX node applies a high voltage pulse between “Signal A” and “Signal B” terminals and the RX node can measure the distance from TX node by evaluating the voltage between these terminals.

In addition to the negative voltage mentioned above, the TX node needs to generate a high voltage pulse since the parasitic capacitance between the nodes is small. To generate the negative voltage and high voltage pulses from a single power supply, this paper uses a charge pump circuit shown in Fig. 8. With this charge pump circuit, a negative voltage of -5V and a high voltage pulse of 10Vp-p can be obtained from a constant 3V DC power supply.

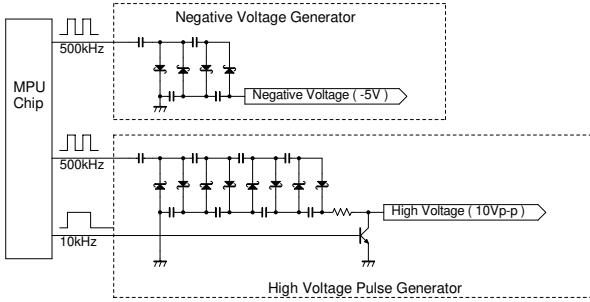


Fig. 8. Charge pump circuit.

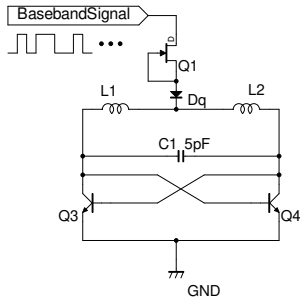


Fig. 9. Equivalent circuit of communication mode.

C. Wireless Communication Mode

The iClay sensor node needs to wirelessly to transmit the obtained distance information to the host computer. When SW is closed in Fig. 2 and digital baseband voltage is applied to “BasebandSignal” terminal, the sensor node enters the wireless communication mode. Fig. 9 shows an equivalent circuit in the communication mode. L1 and L2 are used as the coil of the LC oscillation circuit. Q1 in Fig. 9 acts as a constant current source and Q3 and Q4 behave as negative resistance elements. Therefore, Fig. 9 operates as a Cross Coupled LC Oscillator, and the oscillation frequency is determined by L1, L2, C1 and the drain-source parasitic capacitance of Q2.

The proposed circuit uses the coils for radiation as well as oscillation referring to [11]. The coils are exposed to the outside of the node as shown in Fig. 3, and hence the coil can emit electromagnetic waves in the wireless communication mode and inject pulses in distance sensing mode.

III. EVALUATION

To validate the proposed structure, we evaluate the performance of the sensor node in Figs. 3 and 4 prototyped with discrete components.

A. Wireless Power Supply Mode

As described before, the sensor node should switch to WPS mode automatically when there is no energy left in the node. Therefore, we need to confirm that the sensor node to which no voltages are given from the outside can correctly receive energy wirelessly.

Fig. 10 shows the positional relationship between the power transmission coil and the sensor node. Here, the distance between the power transmission coil and the center of the sensor node was fixed to 20 mm and the voltage between

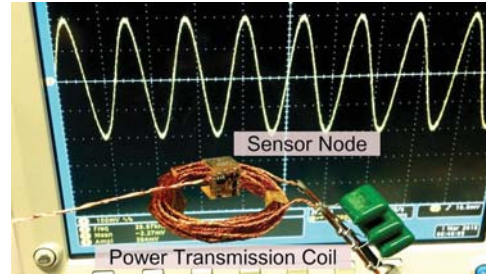


Fig. 10. Experiment of wireless power supply.

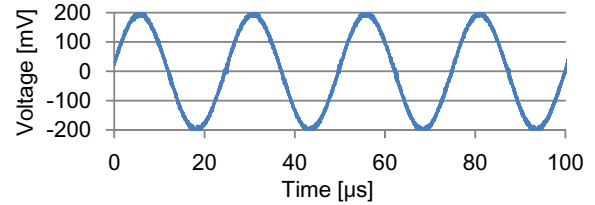


Fig. 11. Output signal of sensor node.

“Signal A” and “Signal B” terminals in Fig. 2 was evaluated with an oscilloscope whose input impedance was $1M\Omega$. Fig. 11 shows the output voltage of the sensor node when a 60Vp-p 40kHz signal is applied to the power transmission coil. We can see that the sensor node outputs a 400 mVp-p sine wave. This result confirms that Q2 in Fig. 2 automatically becomes on and the sensor node enters the wireless power supply mode when there is no power supply. The power consumed by the power transmission coil was 6.5W while the received power was 80 nW. The power supply efficiency is very low. In the iClay system, on the other hand, one wireless transmission coil powers thousands of sensor nodes. Therefore, the conventional metric of power supply efficiency is not suitable for the iClay system. Instead, the total power received by all the nodes should be evaluated, which is included in our future work.

B. Wireless Communication Mode

To confirm that the sensor node can generate a carrier wave for wireless communication, SW in Fig.2 is closed and 3V constant signal is applied to the “BasebandSignal” terminal. For minimizing the influence of measurement on the oscillation, a loop coil was located near the sensor node, and the oscillation signal was evaluated by measuring the voltage induced at the loop coil. The measured waveform in Fig. 12 indicates that the sensor node can generate a carrier wave with a frequency of 102 MHz. The structure of Fig. 2 can perform On-Off-Keying (OOK) modulation by inputting the baseband signal to the “BasebandSignal” terminal. A demodulation experiment was carried out as follows. A super heterodyne type receiver of Fig. 13 was installed 10cm away from the sensor node and a baseband signal with a communication speed of 1kbps was input to the sensor node. The receiver performs frequency conversion, intermediate frequency amplification, and then demodulates the signal using a rectifier circuit and a comparator circuit. The measurement results in Fig. 14 show

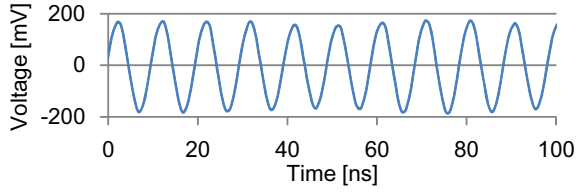


Fig. 12. Measured output of wireless communication mode.

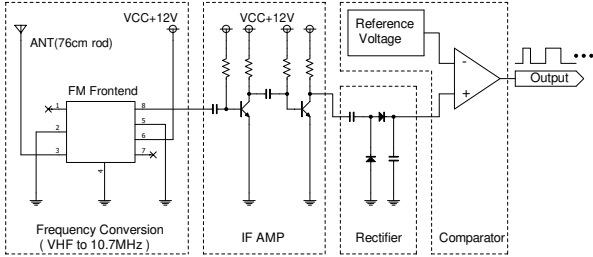


Fig. 13. Schematic of receiver.

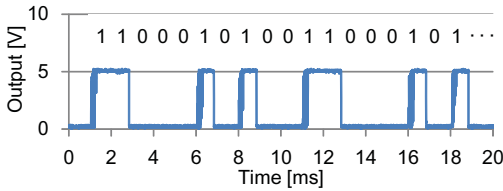


Fig. 14. Waveform at receiver in case of 1kbps communication.

that the symbol string consisting of 1 and 0 can be correctly demodulated, which clarifies the capability of wireless communication. Besides, when the node is communicating at 1 kbps, the energy consumption per bit is 2.1 $\mu\text{J}/\text{b}$. This large energy consumption is due to the low communication speed and energy loss at Q1 and Q2. Even when a voltage of 3V is applied to the sensor node, the potential at the drain and source of Q2 is only 500mV. A voltage drop of 2.5V arises in Q1 and Q2, and consequently, 5/6 of the energy is lost. Minimizing the energy loss at these components is one of our future work.

C. Distance Sensing Mode

As explained in Sec. II-B, high voltage pulses are required for distance sensing, and in this paper, the charge pump circuit in Fig. 8 generates high voltage pulses. The generated high voltage pulses are shown in Fig. 15. The amplitude is 10 V_{p-p}, and the frequency is 10kHz. When the TX node injected this pulse to the electrodes, the signal in Fig. 16 was induced at the RX node located 15 mm away from the TX node. Here, the signal in Fig. 16 contains a lot of noise coming from the charge pump circuit in the RX node. Fig. 17 shows the waveform after this noise is removed by digital signal processing. After the noise removal, we can see that the amplitude varies depending on the inter-node distance d . Fig. 18 depicts the relationship between the node-to-node distance and the peak-to-peak voltage of the received signal. As the distance increases, the peak-to-peak value of the received signal decreases, which means that the proposed sensor node can perform capacitive coupling based inter-node distance sensing.

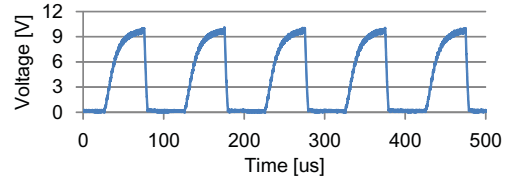


Fig. 15. Signal applied to electrodes at TX node.

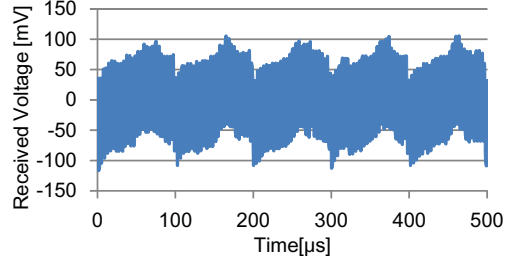


Fig. 16. Received voltage at 15mm away from TX node.

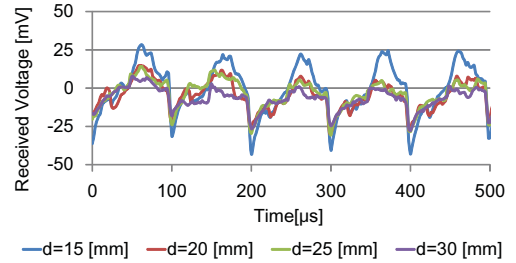


Fig. 17. Measured voltage at RX node (noise canceled.)

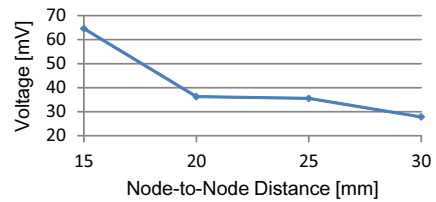


Fig. 18. Distance vs measured voltage amplitude.

IV. CONCLUSION

In this paper, we proposed a sensor node structure in which the functions of WPS, wireless communication, and inter-node distance sensing shared two coils through switching the coil connection. Adopting JFET as the switching element enables to connect two coils even when the node is out of energy, realizing a structure that automatically switches to the WPS mode. These coils can be also used as an oscillation coil and radiation antenna during wireless communication mode. The prototype measurement shows that 1 kbps communication is possible at a distance of 10 cm. Also, it is experimentally confirmed that capacitive coupling based inter-node distance measurement can be performed in a range of 30 mm by disconnecting the two coils.

ACKNOWLEDGEMENTS

This work was supported by JSPS KAKENHI Grant Number JP15H01679.

REFERENCES

- [1] D. Blaauw et al., "IoT design space challenges: Circuits and systems," *Symposium on VLSI Circuits Digest of Technical Papers*, pp. 1–2, June 2014.
- [2] N. Ianuale, D. Schiavon, and E. Capobianco, "Smart cities, big data, and communities: Reasoning from the viewpoint of attractors," *IEEE Access*, vol. 4, pp. 41–47, 2016.
- [3] J. Charthad, N. Dolatsha, A. Rekhi and A. Arbabian, "System-level analysis of far-field radio frequency power delivery for mm-sized sensor nodes," *IEEE Transactions on Circuits and Systems I: Regular Papers*, vol. 63, no. 2, pp. 300–311, Feb. 2016.
- [4] J. Liu, K. Xiong, P. Fan, and Z. Zhong, "RF energy harvesting wireless powered sensor networks for smart cities," *IEEE Access*, vol. 5, pp. 9348–9358, 2017.
- [5] T. Shinada, M. Hashimoto and T. Onoye, "Proximity distance estimation based on capacitive coupling between 1mm^3 sensor nodes," *Analog Integrated Circuits and Signal Processing*, vol. 85, no. 3, pp.425–432, Aug. 2015.
- [6] S. Ukawa, T. Shinada, M. Hashimoto, Y. Itoh, and T. Onoye, "3D Node Localization from Node-To-Node Distance Information Using Cross-Entropy Method," *Proceedings of Virtual Reality Conference* , pp. 303–304 Mar. 2015.
- [7] K. Hirose, S. Ukawa, Y. Itoh, T. Onoye, and M. Hashimoto, "GPGPU-Based Highly Parallelized 3D Node Localization for Real-Time 3D Model Reproduction," *Proceedings of International Conference on Intelligent User Interfaces* , pp. 173–178, Mar. 2017.
- [8] Y. Akihara, T. Hirose, Y. Tanaka, N. Kuroki, M. Numa, and M. Hashimoto, "A Wireless Power Transfer System for Small-Sized Sensor Applications," *Proceedings of International Conference on Solid State Devices and Materials* , pp. 154–155, Sep. 2015.
- [9] S. Masuda, T. Hirose, Y. Akihara, N. Kuroki, M. Numa, and M. Hashimoto, "Highly-Efficient Power Transmitter Coil Design for Small Wireless Sensor Nodes," *Proceedings of International Symposium on Antennas and Propagation*, pp. 512–513, Oct. 2016.
- [10] R. Shirai, J. Kono, T. Hirose, and M. Hashimoto, "Near-field dual-use antenna for magnetic-field based communication and electrical-field based distance sensing in mm^3 -class sensor node," *Proceedings of IEEE International Symposium on Circuits and Systems*, pp. 124–127, May 2017.
- [11] R. Shirai, T. Hirose, and M. Hashimoto, "Dedicated antenna less power efficient OOK transmitter for mm-cubic IoT nodes," *Proceedings of the 47th European Microwave Conference*, pp. 101–104, Oct. 2017.